한국기계가공학회지, 제17권, 제4호, pp.23～31(2018.08) ISSN 1598-6721(Print)
Journal of the Korean Society of Manufacturing Process Engineers, Vol. 17, No. 4, pp.23~31(2018.08) ISSN 2288-0771(Online)

https://doi.org/10.14775/ksmpe.2018.17.4.023

# Stress Analysis and Evaluation of Steam Separator of Heat Recovery Steam Generator (HRSG)

Boo-Youn Lee*,#

*Dept. of Mechanical & Automotive Engineering, KEIMYUNG UNIV.

# 배열회수보일러 기수분리기의 응력해석 및 평가

이부윤*,#

*계명대학교 기계자동차공학전공

(Received 9 May 2018; received in revised form 24 May 2018; accepted 31 May 2018)

## ABSTRACT

Stress of a steam separator, equipment of the high-pressure (HP) evaporator for a HRSG, was analyzed and evaluated according to ASME Boiler & Pressure Vessel Code Section VIII Division 2. First, from the analysis results of the piping system model of the HP evaporator, reaction forces of the riser tubes connected to the steam separator, i.e., nozzle loads, were derived. Next, a finite element model of the steam separator was constructed and analyzed for the design pressure and the nozzle loads. The results show that the maximum stress occurred at the bore of the riser nozzle. The primary membrane stresses at the shell and nozzle were found to be less than the allowable stress. Next, the steam separator was analyzed for the steady-state operating conditions of operating pressure, operating temperature, and nozzle loads. The maximum stress occurred at the bore of the riser nozzle. The primary plus secondary membrane plus bending stress at the shell and nozzle was found to be less than the allowable stress.

**Key Words :** Heat Recovery Steam Generator(배열회수보일러), High Pressure Evaporator(고압증발기), Steam Separator(기수분리기), Stress Analysis(응력해석)

## 1. Introduction

A combined cycle power plant (CCPP) primarily produces power by operating gas turbines that use fuels such as natural gas, followed by producing power secondarily by operating steam turbines with steam made by boiling water using the exhaust gas from the gas turbine. The heat recovery steam generator (HRSG), which is one of the CCPP's core facilities, plays a role as a boiler that produces steam by recovering heat from the exhaust gas emitted from the gas turbines. Thus, all components that make up the HRSG have to be designed safely so as not to be damaged under pressure and thermal loads due to high temperature or pressure[1].

The structural integrity of unfired pressure vessels such as HRSGs are evaluated by applying technical standards such as an ASME Boiler and Pressure Vessel Code Section VIII Division 2[2](ASME code) in the USA and EN13445-3[3](EN code) in Europe.

# Corresponding Author : bylee@kmu.ac.kr
Tel: +82-53-580-5922, Fax: +82-53-580-5165

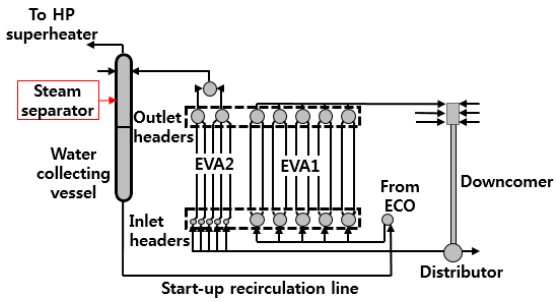


**Fig. 1 Flow diagram of HP evaporator in HRSG**

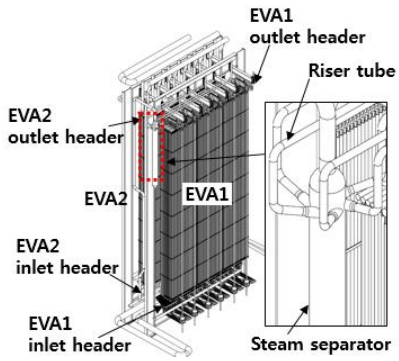


**Fig. 2 Configuration of HP evaporator and steam separator**

This study targets a steam separator, which is one of the pressure vessels that make up a high-pressure (HP) evaporator (EVA) in a Benson-type HRSG[4]. The HP EVA in the Benson-type HRSG consists of two evaporators: EVA1 and EVA2, as shown in the flowchart of Fig. 1. The saturated water introduced from the outlet header of EVA1 is distributed to the inlet headers of EVA2 through the distributor after descending via the downcomer. The steam separator plays the role of separating the steam and moisture as it is installed at the outlet of EVA2. The separated steam is directed to the superheater and the remaining saturated water is transferred to the suction side in the feedwater pump through the water collecting vessel, and this is recirculated as supplied water. This study aims to analyze the stress in the design condition and the steady-state operating conditions in the steam separator in the HP EVA of a Benson-type HRSG to evaluate its safety.

The following previous studies have been conducted in relation to the stress analysis and evaluation of HRSG devices. Chong et al.[5] studied the stress behavior of the superheater tube bundle according to the load-changing operation of the HRSG. Kim et al.[6] analyzed a flow field to evaluate how its fatigue life[7,8] was affected by random vibration of the bumper for vibration prevention in the HRSG's internal tube bundle. Chong et al.[9] examined the technical standards and operation type that affects the fatigue damage to devices of the HRSG, and proposed a method to calculate the damage. Lee[10] evaluated the stress and fatigue in a HP drum in the HRSG by applying the EN Code. Lee[11] evaluated the safety of corrosion fatigue based on the results obtained after transient thermal stress analysis was conducted with regard to the HP drum in the HRSG. Lee[12,13] applied the ASME code to evaluate the structural integrity of the HP EVA's tube bundle and the HP header and distributor in the HRSG.

The steam separator in this study is a pressure vessel, which is long in the vertical direction, as shown in Fig. 2. Six tubes that introduce saturated water from the EVA2 outlet header are radially connected at the upper end of the cylindrical shell. Thus, large stress is generated locally due to the stress concentration at the nozzle where the tubes are connected when the pressure and thermal loads of the design condition are applied. Thus, it is necessary to verify the safety according to the technical standards when the steam separators were designed. This study evaluates the conformance to the design through stress analysis of the design conditions and steady-state condition in accordance with the ASME code regarding the steam separator. A finite element model of the steam separator was made for this and a static structural analysis was conducted using ANSYS[14]. This study evaluated whether the membrane stress and membrane plus bending stress at the shell and nozzle cross-section satisfied the acceptance criteria of the ASME code

at the nozzle bore where the maximum stress was occured due to the stress concentration, which was determined from the analysis results.

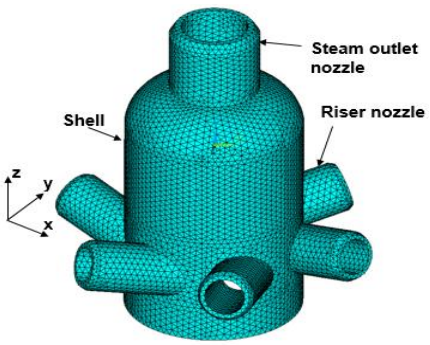


**Fig. 3 Finite element model of steam separator**

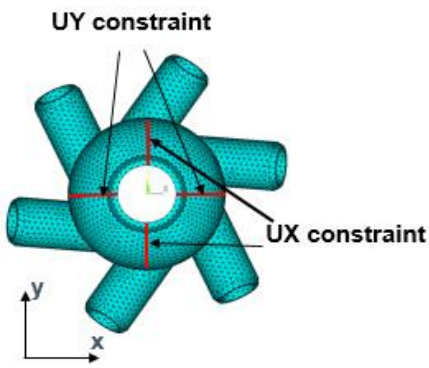


**Fig. 4 Constraint of horizontal displacement**

**Table 1 Material properties of shell and steam outlet nozzle**

| Temp. (°C) | Young's modulus (GPa) | Poisson's ratio | Linear expansion coeff. ($10^{-6}$/K) | Density (kg/m$^3$) |
|---|---|---|---|---|
| 21 | 200 | 0.3 | 6.41 | 7850 |
| 93 | 197 | 0.3 | 6.53 | 7842 |
| 150 | 193 | 0.3 | 6.73 | 7828 |
| 205 | 190 | 0.3 | 6.95 | 7796 |
| 260 | 186 | 0.3 | 7.12 | 7779 |
| 315 | 181 | 0.3 | 7.30 | 7739 |
| 371 | 174 | 0.3 | 7.49 | 7723 |
| 425 | 165 | 0.3 | 7.66 | 7719 |
| 482 | 153 | 0.3 | 7.84 | 7689 |
| 538 | 139 | 0.3 | 8.03 | 7664 |

## 2. Finite element modeling of the steam separator

The finite element model, which was created to analyze the stress of the steam separator, is shown in Fig. 3. A long cylinder in the vertical direction was modeled after separating the upper part where the nozzle was located in consideration of the stress concentration that occurred at the nozzle. The cylindrical shell, which is the main body of the steam separator, has a 610 mm outer diameter and is 52 mm thickness. The nozzle in the vertical direction that connects to the shell's upper end is a steam outlet whose dimensions are 310 mm outer diameter, 40 mm thickness, and 530 mm length. The six nozzles that connect radially to the shell's side are riser nozzles of dimension 195 mm outer diameter, 27.5 mm thickness, and 349 mm length. The finite element mesh was created using the automatic element generation function in ANSYS, and SOLID187, which is a quadratic tetrahedral element, was used to avoid inaccuracy in the stress of the linear tetrahedral element. The total number of elements in the finite element model was 82,337, and the total number of nodes was 135,272.

The displacement in the z-axis direction in the cylindrical shell's bottom surface was restrained as the boundary condition in the vertical direction. The boundary conditions in the horizontal direction was a cross-section that was vertical to the x-axis and restrained the displacement in the y-axis direction and a cross-section that was vertical in the y-axis and restrained the displacement in the x-axis direction with regard to the hemispherical head portion and steam outlet nozzle in the shell's upper end, as shown in Fig. 4.

The material of the cylindrical shell and steam outlet nozzle was SA335-P22, and that of the riser nozzle was SA182-F11 CL2. The design temperature, design pressure, operating temperature, and operating pressure of the steam separator were 423.9°C, 15.5 MPa, 404.4°C, and 13.6 MPa, respectively. The varying values of the physical

properties and allowable stress for each material according to the temperature are presented in the ASME Boiler and Pressure Vessel Code Section II Part D[15]. The physical properties of the shell and steam outlet nozzle (SA335-P22) are summarized in Table 1, and those of the riser nozzle (SA182-F11 CL2) are presented in Table 2. Table 3 presents the allowable stress at the design temperature (423.9°C) and operating temperature (404.4°C) that is required to evaluate the stress.

Since only the nozzles connected to the cylindrical shell in the analysis model of the steam separator in Fig. 3 were modeled and tubes were excluded, loads applied due to cut pipes should be applied to the nozzle cross-section in which six riser tubes were connected radially to the shell side. This load is called the nozzle load in the ASME code. The nozzle load applied to the analysis model of the steam separator is described below.

In a previous study[10], the entire piping system analysis model in the HP EVA was configured as shown in Fig. 5, and static structural analysis was conducted with regard to the entire load (design pressure, design temperature, and dead weight) using ANSYS. The steam separator in the piping system analysis model was modeled with SHELL63, which was a four-node shell element, to consider the cylindrical shape as shown in Fig. 6, and the riser tubes were modeled with PIPE16, which was a two-node pipe element, to enable the extraction of the nozzle load at the riser tube cross-section.

**Table 2 Material properties of riser nozzle**

| Temp. (°C) | Young's modulus (GPa) | Poisson's ratio | Linear expansion coeff. ($10^{-6}$/K) | Density (kg/m$^3$) |
|---|---|---|---|---|
| 21 | 217 | 0.3 | 6.41 | 7850 |
| 93 | 213 | 0.3 | 6.53 | 7842 |
| 150 | 210 | 0.3 | 6.73 | 7828 |
| 205 | 199 | 0.3 | 6.95 | 7796 |
| 260 | 196 | 0.3 | 7.12 | 7779 |
| 315 | 193 | 0.3 | 7.30 | 7739 |
| 371 | 188 | 0.3 | 7.49 | 7723 |
| 425 | 185 | 0.3 | 7.66 | 7719 |
| 482 | 180 | 0.3 | 7.84 | 7689 |
| 538 | 176 | 0.3 | 8.03 | 7664 |

**Table 3 Allowable stresses (unit: MPa)**

| Parts | Allowable stress $S$ | |
|---|---|---|
| | Design temperature | Operating temperature |
| Shell & steam outlet nozzle | 114.0 | 116.0 |
| Riser nozzle | 133.1 | 135.6 |

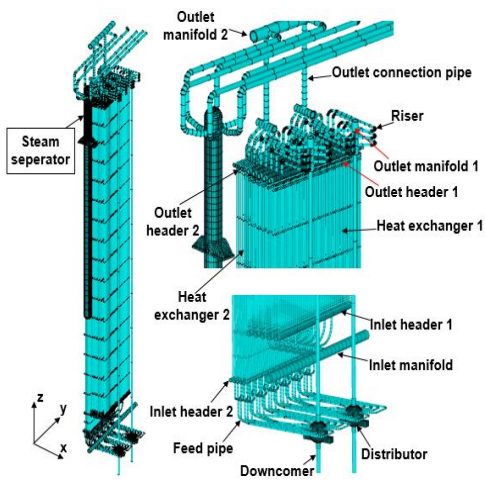


**Fig. 5 Finite element model of piping system of HP evaporator**[12]

The force and moment applied to the riser nozzle cross-section of N1−N6 obtained from the results in the piping system analysis model was the nozzle load that was applicable to the analysis model of the steam separator in Fig. 3.

Table 4 summarizes the extracted results of the nozzle load (force components FX, FY, and FZ and moment components MX, MY, and MZ in the x, y, and z directions, respectively) applied to the riser nozzle of the steam separator from the analysis results of the piping system analysis model. The nozzle load was used as the load applied to the nozzle's cross-section during stress analysis using the analysis model of the steam separator without tubes in the next section.

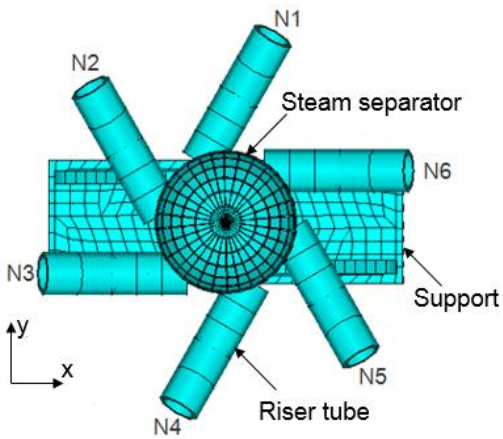


**Fig. 6 Riser tubes connected to steam separator in piping system model**

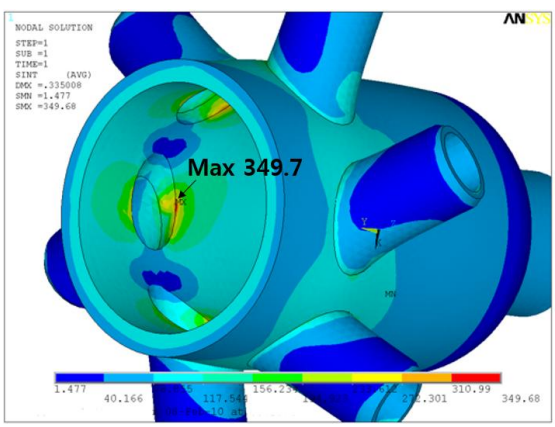


**Fig. 7 Distribution of stress intensity of steam separator under design condition**

**Table 4 Results of nozzle loads of steam separator from piping system model (unit: N, Nm)**

| | FX | FY | FZ | MX | MY | MZ |
|---|---|---|---|---|---|---|
| N1 | -20,299 | -15,017 | 5,725 | 10,010 | -8,882 | 14,466 |
| N2 | -37,806 | 17,619 | 15,281 | -4,751 | 379 | -7,972 |
| N3 | -4,011 | 49,414 | 17,524 | -22,301 | 13,906 | -29,093 |
| N4 | 19,491 | 14,111 | 5,983 | -11,145 | 10,771 | -3,713 |
| N5 | 9,251 | -4,378 | 5,303 | -1,106 | 1,608 | 5,247 |
| N6 | 670 | -9,286 | 5,045 | -917 | 1,168 | 7,787 |

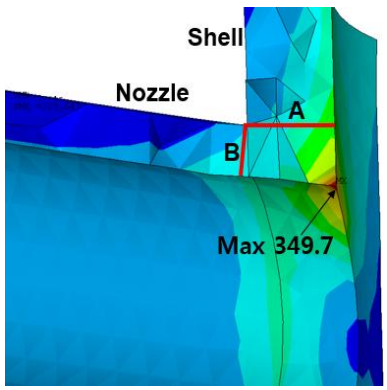


**Fig. 8 Definition of paths A and B for stress linearization under design condition**

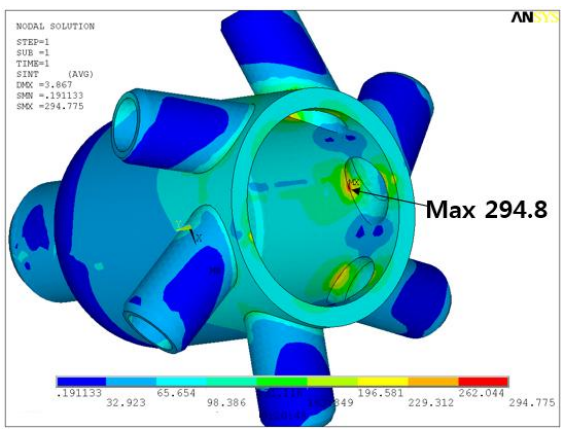


**Fig. 9 Distribution of stress intensity of steam separator under operating condition**

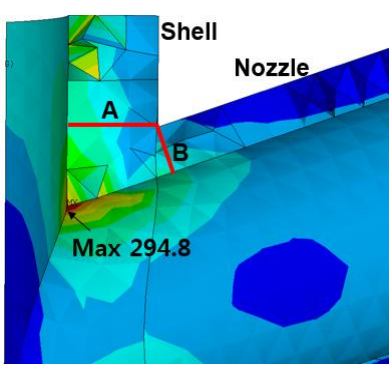


**Fig. 10 Definition of paths A and B for stress linearization under operating condition**

**Table 5 Summary of evaluation of steam separator under design condition (unit: MPa)**

| Path | $P_L$ | $1.5S$ |
|---|---|---|
| A (shell) | 104.5 | 171.0 |
| B (nozzle) | 95.6 | 199.7 |

**Table 6 Summary of evaluation of steam separator under operating condition (unit: MPa)**

| Path | $P_L+P_b+Q$ | $3S$ |
|---|---|---|
| A (shell) | 145.9 | 348.0 |
| B (nozzle) | 104.8 | 406.6 |

## 3. Stress analysis and evaluation of the steam separator

The design condition was analyzed using the finite element model of the steam separator as explained in the previous section. The load in the design condition (with 15.5 MPa design pressure) was applied to the inside surface uniformly and the nozzle load was applied. For the physical properties during the analysis of the design condition, values at the design temperature (423.9°C) were applied in Tables 1 and 2.

Fig. 7 shows the analysis results at the design condition that depict the distribution of stress intensity (referred to as SINT in ANSYS). The maximum stress, which was 349.7 MPa, was generated at the corner of the riser bore inside the shell.

The stress evaluation criteria of the design condition in the ASME code specify the allowable limits of stress intensity($P_m$, $P_L$, and $P_b$) by mechanical loads (primary load) such as pressure, as presented in Eq. (1). $P_m$ refers to the general primary membrane stress excluding the effect of stress concentration and discontinuity, $P_L$ refers to the local primary membrane stress excluding the effect of stress concentration, although a discontinuity is taken into consideration, and $P_b$ refers to the bending stress excluding the effect of discontinuity and stress concentration.

$$\begin{aligned} P_m &\le S \\ P_L &\le 1.5S \\ P_L+P_b &\le 1.5S \end{aligned} \qquad (1)$$

Here, $S$ refers the allowable stress of the material. For the allowable stress $S$ during the evaluation of the design condition, values at the design temperature (as presented in Table 3) should be applied.

The first and third criteria of Eq. (1) are basically satisfied because the thicknesses of the shell and tube are generally determined to satisfy the acceptance criteria of the general primary membrane stress ($P_m$) and bending stress ($P_b$) at the initial design phase of pressure vessel. Thus, it would be sufficient to evaluate whether the second criterion $P_L \le 1.5S$ in Eq. (1) is satisfied by calculating the membrane stress where stress concentration occurs such as at the nozzle portion conservatively when evaluating the finite element analysis results regarding the design condition[10].

The membrane stress($P_m$ or $P_L$) and bending stress($P_b$) that are required during the safety evaluation in accordance with the ASME code such as Eq. (1) can be calculated using the stress linearization function of the post-processor in ANSYS. The path that passes across the thickness of the shell in the pressure vessel is defined and the stress is linearized. Then, the stress is numerically integrated along the path, thereby calculating the linear bending stress that is equivalent to the numerically integrated results of the stress moment and membrane stress (mean stress at the shell thickness).

Fig. 8 indicates Paths A and B, which are set for stress linearization in the nozzle bore where the

maximum stress occurs to evaluate the stress at the design condition. Path A refers to the thickness of the cylindrical shell, and the allowable stress $S$ at the design temperature is 114.0 MPa. Path B refers to the thickness of the riser nozzle, and the allowable stress $S$ at the design temperature is 133.1 MPa.

The results of membrane stress $P_L$ are calculated by performing stress linearization at Paths A and B using a post-processor in ANSYS and are summarized in Table 5 and then compared to the allowable limit $1.5S$. As presented in Table 5, $P_L$ does not exceed $1.5S$ in either the shell or nozzle in the design condition, which verifies the satisfaction of the evaluation criteria for the ASME code.

Next, the steady-state operating condition was analyzed with regard to the steam separator. For the loads, the thermal load, pressure load, and nozzle load at the operating condition were applied. For the thermal load, the operating temperature (404.4°C) was applied uniformly in all the nodes in the steam separator, and the operating pressure (14.6 MPa) was applied uniformly to the inside for the pressure load. The values at the operating temperature (404.4°C) in Tables 1 and 2 were applied to determine the physical properties during the analysis at the operating condition.

In the ASME code, the allowable limit of the range of primary plus secondary stress $P_L+P_b+Q$ due to the mechanical load (primary load) and thermal load (secondary load) between two arbitrary normal operating conditions, i.e., $\Delta(P_L+P_b+Q)$ is specified as presented in Eq. (2). $Q$ refers to the secondary membrane plus bending stress considering discontinuity amd excluding the local stress concentration.

$$\Delta(P_L+P_b+Q) \le 3S \tag{2}$$

where the value at the operating temperature (as presented in Table 3) should be applied for the allowable stress $S$.

The range between the stress at the steady-state operating condition and stress (= 0) at the stationary state of operation in this study was the same as the stress at the steady-state operating condition. Thus, $\Delta(P_L+P_b+Q)$ can be substituted instead of $P_L+P_b+Q$ in the left term of Eq. (2).

Fig. 9 shows the analysis results during the steady-state operating condition, which depicts the distribution of stress intensity. The maximum stress, which was 294.8 MPa, was generated at the corner of the riser bore inside the shell.

$P_L+P_b+Q$ can be calculated using the stress linearization function in the post-processor of ANSYS. Fig. 10 indicates Paths A and B, which are set for the stress linearization in the nozzle bore where the maximum stress occurs to evaluate the stress at the steady-state operating condition. Path A refers to the thickness of the cylindrical shell and the allowable stress $S$ is 116.0 MPa at the operating temperature. Path B refers to the thickness of the riser nozzle and allowable stress $S$ when the operating temperature is 135.6 MPa. The results of the primary plus secondary membrane plus bending stress $P_L+P_b+Q$ calculated by performing stress linearization at Paths A and B using a post-processor of ANSYS are summarized in Table 6 and compared with the allowable limit $3S$. As presented in Table 6, $P_L+P_b+Q$ does not exceed $3S$ in either the shell or nozzle in the steady-state operating condition, which verifies the satisfaction of the evaluation criteria of the ASME code.

## 4. Conclusion

This study performed a structural analysis of the design and steady-state operating conditions with

regard to the steam separator of the HP EVA in the HRSG and evaluated the design conformance in accordance with the ASME code, which was a technical standard. This study's conclusions are summarized as follows:

1. The nozzle load of the riser that was connected radially to the side of the steam separator was derived from the analysis results of the piping system in the HRSG. This nozzle load was used as a load applied to the nozzle cross-section during the stress analysis of the steam separator.
2. The analysis model of the steam separator was created and static structural analysis was conducted with regard to the design condition. The maximum stress occurred at the corner of the rise nozzle bore. The local primary membrane stress at the maximum stress location was 104.5 MPa at the shell and 95.6 MPa in the nozzle, which were smaller than the respective acceptance criteria of 171.0 MPa and 199.7 MPa. Thus, both satisfied the acceptance criteria of the ASME code.
3. The static structural analysis was conducted with regard to the analysis model of the steam separator. The maximum stress occurred at the corner of the rise nozzle bore. The primary plus secondary membrane plus bending stress at the maximum stress location was 145.9 MPa in the shell and 104.8 MPa in the nozzle, which were smaller than the respective acceptance criteria of 348.0 MPa and 406.6 MPa; thus, both satisfied the acceptance criteria of the ASME code.
4. The stress analysis, safety evaluation method, and actual applied case study of the steam separator in the HP EVA according to the ASME code presented in this study are expected to be utilized in the design verification process for similar devices. The fatigue evaluation of the steam separator under the transient operating conditions, which was not discussed in this study, will be presented in a future study.

## REFERENCES


1. Eriksen, V. R., Heat Recovery Steam Generator Technology, Woodhead Publishing, 2017.
2. ASME Boiler and Pressure Vessel Code Section VIII Division 2: Alternate Rules, Rules for Construction of Pressure Vessels, American Society of Mechanical Engineers, 2010.
3. EN 13445-3:2009, Unfired Pressure Vessels - Part 3: Design, European Committee for Standardization, 2009.
4. Volpi, G., Penati, M. and Silva, G., "Heat Recovery Steam Generators for Large Combined Cycle Plants (250 MWe GT Output): Experiences with Different Design Options and Promising Improvements by Once-through Technology Development," Proc. of Power Gen Europe 2005, Milan, 28-30 June, 2005.
5. Chong, C. H. and Song, J. I., "Stress Behaviors of Superheater Tubes under Load Change Operation in HRSG," Journal of the Korean Solar Energy Society, Vol. 28, No. 6, pp. 33-39, 2008.
6. Kim, J. B., Hwang, S. H. and Chung, J. C., "The CFD Analysis for the Fatigue Life Evaluation of HRSG Bumper," Proc. of KSME Autumn Conference, pp. 1280-1285, 2015.
7. Shin. Y. J., Choi, C. H., Lee, S. G. and Kim, J. H., "Fatigue CAE Analysis of a Rebar Bending Machine Roller," Journal of the Korean Society of Manufacturing Process Engineers, Vol. 14, No. 2, pp. 75-80, 2015.
8. Cho, S. J., Park, Y. J., Han, J. W. and Lee, G. H., "Fatigue Life Prediction of the Carrier of Slewing Reducer for Tower Crane," Journal of the Korean Society of Manufacturing Process Engineers, Vol. 14, No. 3, pp. 131-140, 2015.
9. Chong, C. H., Kim, H. G., Choi, Y. J., Lee, C. S. and Ha, J. W., "Design Life Analysis for HRSG," Proc. of KSME Autumn Conference, pp. 55-60, 2004.

10. Lee, B. Y., “Evaluation of Stress and Fatigue of High-Pressure Drum for Heat Recovery Steam Generator According to European Code,” Transaction of the Korean Society of Mechanical Engineers A, To be published, Vol. 42, No. 9, 2018.
11. Lee, B. Y., “Evaluation of Safety of Corrosion Fatigue of High Pressure Drum for Heat Recovery Steam Generator Using Transient Thermal Stress Analysis,” Journal of the Korean Society of Precision Engineering, To be published, Vol. 35, No. 10, 2018.
12. Lee, B. Y., “Evaluation of Stress and Fatigue Life of Tube Bundle and Header for High-Pressure Evaporator of Heat Recovery Steam Generator,” Trans. KSME A, Submitted, 2018.
13. Lee, B. Y., “Stress and Fatigue Evaluation of Distributor for Heat Recovery Steam Generator in Combined Cycle Power Plant,” Journal of the Korea Academia-Industrial Cooperation Society, Accepted, 2018.
14. ANSYS, ANSYS User’s Manual Version 11, ANSYS Inc., 2007.
15. ASME Boiler and Pressure Vessel Code Section II Part D: Materials Properties, American Society of Mechanical Engineers, 2010.